Non-causal Linear Optimal Control with Adaptive Sliding Mode Observer for Multi-Body Wave Energy Converters

Yao Zhang, Peter Stansby, Guang Li *Member, IEEE*

Abstract—As a non-causal optimal control problem, the performance of wave energy converter (WEC) control relies on the accuracy of the future incoming wave prediction. However, the inevitable prediction errors can degrade WEC performance dramatically especially when a long prediction horizon is needed by a WEC non-causal optimal controller. This paper proposes a novel non-causal linear optimal control with adaptive sliding mode observer (NLOC+ASMO) scheme, which can effectively mitigate the control performance degradation caused by wave prediction errors. This advantage is achieved by embedding the following enabling techniques into the scheme: (i) an adaptive sliding mode observer (ASMO) to estimate current excitation force in real-time with explicitly formulated boundary of estimation error, (ii) an auto-regressive (AR) model to predict the incoming excitation force with explicitly formulated boundary of prediction error using a set of latest historical data of ASMO estimations from (i), and (iii) a compensator to compensate for both the estimation error and the prediction error of excitation force. Moreover, the proposed NLOC+ASMO scheme does not cause heavy computational load enabling its real-time implementation on standard computational hardware, which is especially critical for the control of WECs with complicated dynamics. The proposed NLOC+ASMO framework is generic and can be applied to a wide range of WECs, and in this paper we demonstrate the efficacy by using a multi-float and multi-motion WEC called M4 as a case study, whose control problem is more challenging than the widely studied point absorbers. Simulation results show the effectiveness of the proposed control scheme in a wide range of sea states, and it is also found that the controller is not sensitive to change of ASMO parameters.

Index Terms—Wave energy converter (WEC), Excitation force estimation and prediction, sliding mode compensator, non-causal linear optimal control (NLOC), M4

I. INTRODUCTION

Sea wave energy is an enormous source of offshore renewable energy with high energy density [1]. Many types of wave energy converters (WECs) have been designed to harness the wave power [2], such as point absorbers, oscillating water columns, overtopping devices and attenuators, etc.

Y. Zhang is with School of Mechanical and Construction Engineering, Northumbria University, NE1 8ST, U.K. e-mail: yaozhanghit@outlook.com.

G. Li is with School of Engineering and Materials Science, Queen Mary University of London, E1 4NS, U.K. e-mail: g.li@qmul.ac.uk.

P. Stansby is with the Department of Mechanical, Aerospace and Civil Engineering, University of Manchester, Manchester, M13 9PL, U.K. email: p.k.stansby@manchester.ac.uk.

Many control strategies have been proposed to maximize the energy output of WECs and maintain their safe operations [3]. The energy maximization control for WECs has been developed from causal control in the early stage [3], [4] to non-causal control in recent studies, such as non-causal linear optimal control (NLOC) [5], model predictive control (MPC) [6]–[9], etc. Non-causal control is a control strategy such that the future information contributes to the current control input. In particular, the non-causal control for WECs is based on the prediction of the incoming wave excitation force or the wave elevation, and it has been recognized that real-time control of WECs benefits from excitation force predictions [10], [11].

The wave prediction methods are mainly divided into two categories: 1) deterministic prediction methods that are based on the measurements at multiple nearby locations around the WECs, such as the deterministic sea wave prediction (DSWP) [12] and 2) statistical methods based on the analysis of the past measurement data using statistical models, such as the Auto-Regressive (AR) model [13]–[16]. In comparison, deterministic methods provide a much longer and reliable prediction horizon of wave profiles but at an increased cost of measurement hardware installation and maintenance. No matter which wave prediction technique is adopted by non-causal WEC control, prediction error is unavoidable and this error grows with the increase of the prediction horizon. Moreover, for some optimal non-causal WEC control strategies, e.g. NLOC and MPC, we normally need a long prediction horizon to approximate the optimal control performance within the computational burden limit. Thus for the applications of these control strategies in many practical cases, the prediction error can significantly degrade the WEC control performance. The sensitivity of non-causal control of WECs to excitation force prediction errors has been analyzed in [17], [18].

In this paper, we aim to develop a robust non-causal linear optimal control framework for WEC control problem to explicitly compensate for the prediction errors caused by statistical wave prediction methods. To achieve non-causal control using the statistical methods with satisfactory performance relies on a combination of a wave force estimation technique with sufficient accuracy and the following prediction method based on a segment of latest historical data produced by the wave estimation. To estimate the excitation force in real-time, extended Kalman filter (EKF) [13], [19], unknown input observer [20] and adaptive sliding mode observer (ASMO) [21] have been proposed to cope with uncertainties with acceptable estimation error. Based on the historical estimations,

AR and EKF have been applied to predict incoming excitation forces [13]–[16].The proposed NLOC+ASMO has its roots in the recent techniques developed in [5], [18], [21]. The enhanced robustness to prediction error is achieved by fusing the following enabling technologies within one framework:

1) an ASMO to estimate current excitation force in real-time with explicitly formulated boundary of estimation error,
2) an online-updated AR model to predict the incoming excitation force using a set of latest historical estimation data with explicitly formulated boundary of prediction error,
3) a real-time sliding mode compensator to mitigate the estimation and prediction error, and
4) the NLOC control strategy [5] to determine optimal control input based on improved accuracy of the estimated and predicted wave excitation forces.

The paper extends the results in [22] and [21] with some novel development. Different from the control method in [22] and [21], the incoming excitation force is obtained by ASMO and AR predictor, and the estimation and prediction error degrading control performance significantly are explicitly taken into account by sliding mode compensator. The advantages and novelties of this method are summarized as follows:

- Only the position and velocity of floats are essential for the proposed strategy (accelerometers are available in practice to give the velocity and position by integrations), which significantly reduces the cost of hardware installations;
- Owing to the novel features of proposed compensator, the prediction error caused by AR is explicitly handled, which effectively avoids control performance degradation and enables long-term predictions without error or with reduced error to contribute to the non-causal LOC performance;
- Since parameters of the proposed control scheme can be determined off line, the proposed method achieves real-time implementations with low computational load, which is of great importance for M-WECs with high number of freedoms and high model order.

To demonstrate the efficacy and effectiveness of the proposed NLOC+ASMO scheme, we apply to a multi-float and multi-motion WEC (M-WEC), although the scheme can be more easily applied to single float WECs. In particular, an attenuator type M-WEC, called M4, is chosen in this paper as a case study to demonstrate the efficacy and effectiveness of the proposed control scheme. Although M4 device has linear hydrodynamic characteristics, controller design for a M-WEC is much more challenging than for a single float WEC, due to the dramatically increased computational burden. As shown in Fig. 1, M4 is based on a reconfigurable design, whose detailed design has been demonstrated in [23]–[26]. A 1:40 laboratory scale geometry of 3-float M4 is shown in Fig. 2. From left to right, the bow float, middle float, stern float, beam connecting bow and middle float, beam connecting middle and stern float, and the power take off unit are indexed from 1 to 6, $i = 1, \cdots, 6$, respectively. For a body interacting with wave, it
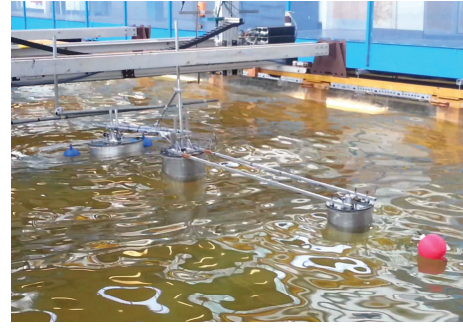

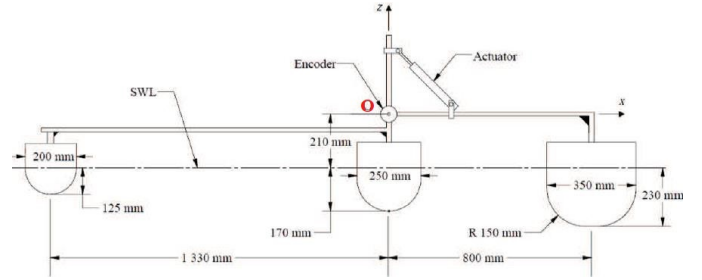Fig. 1.   Tank experiment of M4 in Manchester, UK [23]

Fig. 2.   The schematic diagram of laboratory scale 3-float 1-1-1 M4 [23]

has six degrees of freedom. They are surge, sway, heave, roll, pitch and yaw, noted as mode from 1 to 6, respectively, with sway, roll and yaw not relevant here. A 1-1-1 format M4 is considered in this paper. (Details of M4 design are shown in [23]–[26].) The larger number of floats are being investigated hydrodynamically [23] will provide a future challenge.

The state-space modeling and the non-causal LOC design of M4 have been proposed in [22], which verifies the effectiveness of the non-causal LOC being applied in M-WECs. Based on this work, a generic non-causal LOC integrated with excitation force prediction has been proposed in [16], which applies extended Kalman Filter (EKF) to estimate and predict the wave excitation force, while the control degradation by the prediction error is presented in [16]. Thus this paper can also be seen as an extension of these works by improving these existing WEC control methods.

Notations of this paper are listed in Table I. In the sequel, $x^{(Q)}$ denotes each component of vector x with $Q = x_0, z_0, \theta_1, \theta_2$. $0_{l_1 \times l_2}$ denotes the zero matrix with the size of $l_1 \times l_2$, and I_{l_1} is an identity with the size of l_1. l_1 and l_2 are positive integers. The rest of the paper is organized as follows. Section II includes control-oriented modelof M4 and the existing controller. The proposed control scheme is designed in Section III. Simulation results of the comparison between the proposed controller and the existing method are shown in Section IV. The conclusions are summarized in Section V.

II. Preliminary with Introduction

In this section, notations and the state-space (control-oriented) model of M4 are introduced. The previous result of a non-causal LOC for M4 [22] is briefly recalled, in which the perfect future excitation force is assumed. The requirements

TABLE I
NOTATIONS

Variables in M4 Model

q	$\triangleq$	M4 state vector, $q = \begin{bmatrix} q^{(x_0)} & q^{(z_0)} & q^{(\theta_1)} & q^{(\theta_2)} \end{bmatrix}^{\mathrm{T}}$
$q^{(x_0)}/ q^{(z_0)}$	$\triangleq$	surge/heave position of the hinge O
$q^{(\theta_1)}/ q^{(\theta_2)}$	$\triangleq$	pitch angle of i which is on the left of the hinge O ($i = 1, 2, 4$)/on the right of the hinge O ($i = 3, 5, 6$)
m_s / m_∞	$\triangleq$	M4 mass/added mass, $M := m_s + m_\infty$
K	$\triangleq$	M4 restoring force coefficient matrix
(A_r, B_r, C_r, D_r)	$\triangleq$	state-space representation of radiation force
F_r	$\triangleq$	the convolution term of radiation force
r	$\triangleq$	the $n_r \times 1$ state vector corresponding to the radiation force, no physical meaning
f_u	$\triangleq$	PTO force

Actual Excitation Force/Moment

f_e, w	$\triangleq$	actual wave excitation force, $w = \begin{bmatrix} w^{(x_0)} & w^{(z_0)} & w^{(\theta_1)} & w^{(\theta_2)} \end{bmatrix}^{\mathrm{T}}$
$w^{(x_0)} / w^{(z_0)}$	$\triangleq$	actual surge/heave excitation force
$w^{(\theta_1)} / w^{(\theta_2)}$	$\triangleq$	actual excitation moment of i which is on the left of the hinge O ($i = 1, 2, 4$)/on the right of the hinge O ($i = 3, 5, 6$)
w_{k,n_p}	$\triangleq$	vector of actual future wave excitation force, $w_{k,n_p} = \begin{bmatrix} w_k^{\mathrm{T}} & w_{k+1}^{\mathrm{T}} & \cdots & w_{k+n_p-1}^{\mathrm{T}} \end{bmatrix}^{\mathrm{T}}$
n_p	$\triangleq$	prediction horizon/steps

Estimated Excitation Force/Moment

$\hat{f}_e, \hat{w}$	$\triangleq$	real-time estimation of wave excitation force, $\hat{w} = \begin{bmatrix} \hat{w}^{(x_0)} & \hat{w}^{(z_0)} & \hat{w}^{(\theta_1)} & \hat{w}^{(\theta_2)} \end{bmatrix}^{\mathrm{T}}$
$\hat{w}^{(Q)}$	$\triangleq$	real-time estimation of excitation force along Q component, $Q = x_0, z_0, \theta_1, \theta_2$
$\tilde{f}_e, \tilde{w}$	$\triangleq$	estimation error of wave excitation force, $\tilde{w} = \begin{bmatrix} \tilde{w}^{(x_0)} & \tilde{w}^{(z_0)} & \tilde{w}^{(\theta_1)} & \tilde{w}^{(\theta_2)} \end{bmatrix}^{\mathrm{T}}$
$\tilde{w}^{(Q)}$	$\triangleq$	estimation error of excitation force along Q component, $Q = x_0, z_0, \theta_1, \theta_2$

Predicted Excitation Force/Moment

$\hat{w}_{k+i}$	$\triangleq$	i-step-ahead prediction of wave excitation force, $i = 0, ..., n_p - 1$, $\hat{w}_{k+i} = \begin{bmatrix} \hat{w}_{k+i}^{(x_0)} & \hat{w}_{k+i}^{(z_0)} & \hat{w}_{k+i}^{(\theta_1)} & \hat{w}_{k+i}^{(\theta_2)} \end{bmatrix}^{\mathrm{T}}$
$\hat{w}_{k+i}^{(Q)}$	$\triangleq$	i-step-ahead prediction of excitation force along Q component, $Q = x_0, z_0, \theta_1, \theta_2$
$\hat{w}_{k,n_p}$	$\triangleq$	vector of predicted wave excitation force, $\hat{w}_{k,n_p} = \begin{bmatrix} \hat{w}_k^{\mathrm{T}} & \hat{w}_{k+1}^{\mathrm{T}} & \cdots & \hat{w}_{k+n_p-1}^{\mathrm{T}} \end{bmatrix}^{\mathrm{T}}$
w_{k+i}	$\triangleq$	i-step-ahead actual wave excitation force, $i = 0, ..., n_p - 1$, $w_{k+i} = \begin{bmatrix} w_{k+i}^{(x_0)} & w_{k+i}^{(z_0)} & w_{k+i}^{(\theta_1)} & w_{k+i}^{(\theta_2)} \end{bmatrix}^{\mathrm{T}}$
$w_{k+i}^{(Q)}$	$\triangleq$	i-step-ahead actual excitation force along Q component, $Q = x_0, z_0, \theta_1, \theta_2$
$\tilde{w}_{k+i\|k}$	$\triangleq$	i-step-ahead prediction error of wave excitation force, $i = 0, ..., n_p - 1$, $\tilde{w}_{k+i\|k} = \begin{bmatrix} \hat{w}_{k+i}^{(x_0)} & \tilde{w}_{k+i}^{(z_0)} & \tilde{w}_{k+i}^{(\theta_1)} & \tilde{w}_{k+i}^{(\theta_2)} \end{bmatrix}^{\mathrm{T}}$
$\tilde{w}_{k+i\|k}^{(Q)}$	$\triangleq$	i-step-ahead prediction error along Q component, $Q = x_0, z_0, \theta_1, \theta_2$
$\tilde{w}_{k,n_p}$	$\triangleq$	vector of excitation force prediction error, $\tilde{w}_{k,n_p} = \begin{bmatrix} \tilde{w}_k^{\mathrm{T}} & \tilde{w}_{k+1}^{\mathrm{T}} & \cdots & \tilde{w}_{k+n_p-1}^{\mathrm{T}} \end{bmatrix}^{\mathrm{T}}$

for the designs of observer, predictor and controller for energy maximization of a WEC in real scenario are analyzed, which demonstrate the main motivations of integrating ASMO, AR model and SMC to the non-causal LOC.

A. State-space (control-oriented) model of M4

The dynamic model of M4 [22] is as follows

$$
\begin{cases}
M\ddot{q} = -Kq - f_r + f_e + f_u \\
\dot{r} = A_r r + B_r \dot{q} \\
f_r = C_r r + D_r \dot{q}
\end{cases}
\tag{1}
$$

Define the states as $x_1 := q$, $x_2 := r$ and $x_3 := \dot{q}$. Define the control input (the PTO force) and the disturbance (excitation force) as $u := f_u$ and $w := f_e$ respectively. Define the output (the relative pitch velocity) as $y = \dot{\theta}_1 - \dot{\theta}_2$. Substituting the system state $x = [x_1^{\mathrm{T}} \ x_2^{\mathrm{T}} \ x_3^{\mathrm{T}}]^{\mathrm{T}} = [q^{\mathrm{T}} \ r^{\mathrm{T}} \ \dot{q}^{\mathrm{T}}]^{\mathrm{T}}$ into (1), we have the following state-space model

$$
\begin{cases}
\dot{x} = A_c x + B_{uc} u + B_{wc} w \\
y = C_c x
\end{cases}
\tag{2}
$$

where

$$
A_c = \begin{bmatrix}
0_{4 \times 4} & 0_{4 \times n_r} & I_4 \\
0_{4 \times 4} & A_r & B_r \\
-M^{-1}K & -M^{-1}C_r & -M^{-1}D_r
\end{bmatrix}
$$
$$
B_{uc} = \begin{bmatrix} 0_{4 \times 1} & 0_{n_r \times 1} & M^{-1}[0 \ 0 \ 1 \ -1]^{\mathrm{T}} \end{bmatrix}^{\mathrm{T}}
$$
$$
B_{wc} = \begin{bmatrix} 0_{4 \times 4} & 0_{n_r \times 4} & M^{-1} \end{bmatrix}^{\mathrm{T}}
$$
$$
C_c = \begin{bmatrix} 0_{1 \times 6} & 1 & -1 & 0_{1 \times n_r} \end{bmatrix}
$$

A discrete-time model (2) can be obtained from the continuous-time model by a zero-order hold

$$
\begin{cases}
x_{k+1} = Ax_k + B_u u_k + B_w w_k \\
y_k = Cx_k
\end{cases}
\tag{3}
$$

where (A, B_u, B_w, C) are the discrete-time state space matrices of the corresponding continuous model with matrices $(A_c, B_{uc}, B_{wc}, C_c)$.

B. Problem Introduction

For the WEC control, the main aim is to maximize the energy output by solving the following optimal control problem [5], [22]:

$$
\min_{u_0,...,u_N} \Sigma_{k=0}^{N} \left\{ y_k u_k + \frac{1}{2} x_k^{\mathrm{T}} Q_c x_k + \frac{1}{2} R u_k^2 \right\}
\tag{4}
$$

subject to the state-space model (3), where Q_c and R are positive definite.

For the first term in the cost function, since the power output is $P_k = -y_k u_k$, to minimize $y_k u_k$ is to maximize of power, whose integration is the energy output. The second and third terms are introduced to construct a convex optimization problem and add soft constraints. The second term is to penalize the magnitude of the state vector x_k to ensure safe operations. The third term is to limit the maximal PTO torque by tuning the weight R. As reported in [22], given the accurate information
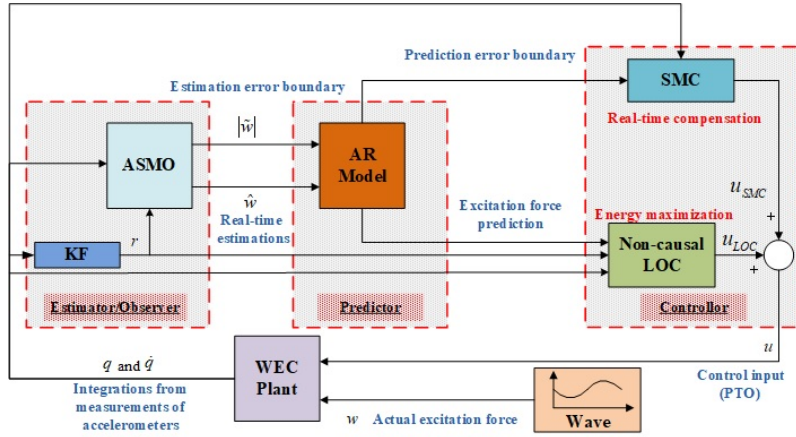
Fig. 3. Block diagram of the proposed control framework

of the incoming excitation force w_{k,n_p}, the solution of the non-causal optimal problem (4) is the non-causal linear optimal control law

$$u_{LOC} = K_x x_k + K_d w_{k,n_p} \qquad (5)$$

where n_p is the wave prediction horizon. K_x and K_d are constant gain parameters to be pre-calculated off-line [5] by $K_x = -(R + B_u^{\mathrm{T}} Y B_u)^{-1}(C + B_u^{\mathrm{T}} Y A)$, $K_d = -(R + B_u^{\mathrm{T}} Y_{k+1} B_u)^{-1} B_u^{\mathrm{T}} \Psi$ and $Y = Q_c + A^{\mathrm{T}} Y A - (C_k + B_u^{\mathrm{T}} Y A)^{\mathrm{T}}(R + B_u^{\mathrm{T}} Y B_u)^{-1}(C + B_u^{\mathrm{T}} Y A)$, where Y is algebraic Riccati equation solution and $\Psi := [Y B_w, \Phi Y B_w, \ldots, \Phi^{n_p-1} Y B_w]$ with $\Phi = (A + B_u K_x)^{\mathrm{T}}$.

C. Requirements in Practical Application

The NLOC (5) provides the optimal solution of energy maximization based on the accurate information of current and future wave excitation force. However, in the real scenario, we enhance the robustness of the NLOC, because wave excitation force estimation and prediction inevitably introduces errors, which degrade the WEC control performance. The requirements of controller and observer design can be summarized as follows:

- The excitation force observer should explicitly formulate the estimation error boundary which enables controller to compensate in order to maintain control performance;
- The prediction method should account for the changes of sea states to provide accurate excitation force predictions. Furthermore, since the control policy applied in this paper is a non-causal control, the prediction method should ensure that the prediction error boundary can be estimated so that it can be compensated for by the non-causal controller;
- The controller should be robust against the inaccurate estimations and predictions of the excitation force.

III. Non-causal Linear Optimal Control with Adaptive Sliding Mode Observer for Energy Maximization

In this section, the overall control scheme is firstly proposed. An ASMO and improved AR model are briefly introduced

which are used for derivation of the estimation error boundary and prediction error boundary, respectively. The proposed NLOC+ASMO is then designed to optimize the WEC energy output using inaccurate estimations and predictions.

A. Overall strategy

As shown in Fig. 3, the overall strategy of the proposed scheme of WEC control are as follows:

- Since the excitation force cannot be measured easily, an observer is proposed to estimate excitation force in real time. The upper boundary of the prediction error is explicitly formulated which enables the proposed compensator to compensate for estimation error.
- Considering that the future wave excitation force is required to contribute to the current control input, the AR method with time-varying coefficients is applied to provide short-term prediction of incoming wave excitation force.
- The prediction error boundary of the excitation force can be obtained by a linear combination of the latest historical prediction error boundaries;
- A compensator is incorporated into the control scheme to explicitly cope with the wave force estimation error and prediction error.

B. Excitation Force Observer Design

To meet the requirement of observer design analyzed in Section II-C, an adaptive sliding mode observer (ASMO) [21] is adopted to estimate wave excitation force in real-time based on the model (1) and (2), and ensures a pre-defined convergence time. The boundary of the estimation error is also calculated.

Assumption 1. *Each components of the wave excitation force and the first time derivatives are bounded, i.e. $|w^{(Q)}| \le F_e^{(Q)}$ and $|\dot{w}^{(Q)}| \le \Omega^{(Q)}$ hold, where $F_e^{(Q)}$ and $\Omega^{(Q)}$ are constants.*

A sliding surface is chosen as $s := \dot{q} - h$, where h is

designed as

$$Mh = \int (u + \hat{w} + \mu_0 s^\alpha + \mu_1 \mathrm{sgn}(s) - Kq - D_r\dot{q} - C_r r)dt \tag{6}$$

where $\hat{w} = [\hat{w}^{(x_0)}, \hat{w}^{(z_0)}, \hat{w}^{(\theta_1)}, \hat{w}^{(\theta_2)}]^{\mathrm{T}}$ is a vector of the estimation, $\mu_0 > 0$ and $\alpha > 1$ are constants and μ_1 is designed as $\mu_1 = \|\hat{w}\| + F_e + k_1$, where $F_e = \max\{F_e^{(Q)}\}$ and $k_1 > 0$ are constants.

The proposed ASMO is designed [21] as

$$\begin{cases} \hat{w} &= \lambda + M\dot{q} \\ \lambda &= \int (Kq + D_r\dot{q} + C_r r - u - \hat{w} + (\hat{\Omega} + K_\mu)\mathrm{sgn}(s))dt \end{cases} \tag{7}$$

where $\lambda \in \mathbb{R}^4$ is an observer internal variable and $K_\mu = \mu_2 I_4$ is a constant matrix with $\mu_2 > 0$ a constant. The definition of the function of $\mathrm{sgn}(\Delta)$ is $\mathrm{sgn}(\Delta) = \begin{cases} \frac{\Delta}{\|\Delta\|}, & \Delta \neq 0 \\ 0, & \Delta = 0 \end{cases}$, $\hat{\Omega} = \mathrm{diag}\{\hat{\Omega}^{(x_0)}, \hat{\Omega}^{(z_0)}, \hat{\Omega}^{(\theta_1)}, \hat{\Omega}^{(\theta_2)}\}$ is the matrix of the boundary estimation of the first derivative of the wave excitation force with respect to time, whose derivative is designed as

$$\dot{\hat{\Omega}}^{(Q)} = -k_2\hat{\Omega}^{(Q)} + 2|\hat{w}^{(Q)}| + 2F_e^{(Q)}, \quad \Omega^{(Q)}(t_0) = 0 \tag{8}$$

where $k_2 > 0$ is a constant.

Lemma 1. *[21]. The estimation error boundary is available by ASMO when $t \geq T_1$ holds, and it can be explicitly calculated by*

$$|\tilde{w}^{(Q)}(t)| \leq \tilde{F}_e^{(Q)}(t) \tag{9}$$

where

$$\tilde{F}_e^{(Q)}(t) = \frac{k_2 + 4k_2(\Omega^{(Q)})^2}{8(1 - \frac{2\Omega^{(Q)} + 2F_e^{(Q)}}{(t - T_1)\min\{2\mu_2, k_2/\sqrt{2}\}})\min\{2\mu_2, k_2/\sqrt{2}\}}$$

and

$$T_1 = \frac{1}{k_1}\lambda_{max}^{\frac{1}{2}}(M) + \frac{1}{\mu_0(\alpha - 1)}\lambda_{max}^{\frac{\alpha+1}{2}}(M)$$

with $\lambda_{max}(M) > 0$ as the largest eigenvalue of the matrix M.

Remark 1. *The period $0 \leq t < T_1$ is a warming-up process allowing the estimation error to be steered into a bound determined by (9). The controller starts to work at $t = T_1$. T_1 is fixed once parameters k_1, μ_0 and α are set.*

Remark 2. *(Parameter tuning guide of ASMO) The parameters k_1, μ_0 and α determine the length of warming-up period. In particular, greater values of k_1 and μ_0 lead to a smaller value of T_1 representing a shorter warming-up period, and $\alpha = \sqrt{2\lambda_{max}(M) + 1}$ leads to the fastest warming-up process, which is obtained by taking the extreme value of the partial derivative.*

C. Wave Excitation Force Prediction

To meet the requirements of the wave excitation force predictor as analyzed in Section II-C, an improved AR model [21] is employed to 1) provide the prediction of the incoming excitation force based on the past estimations and 2) explicitly formulate the prediction error bounds.

One-step-ahead prediction of the excitation force along the Q-component is

$$\hat{w}_{k+1|k}^{(Q)} = \sum_{i=0}^{p-1}(\phi_i \hat{w}_{k-i}^{(Q)}) \tag{10}$$

where p is AR prediction model order, and ϕ_i are the AR model coefficients with $i = 0, 1, ..., p-1$, which are trained online by the latest estimations in order to account for the varying sea states. The l-step-ahead prediction of the excitation force is calculated based on one-step-ahead prediction. The error of one-step-ahead prediction $\tilde{w}_{k+1|k}^{(Q)}$ is

$$|\tilde{w}_{k+1|k}^{(Q)}| = \sum_{j=0}^{p-1}(\phi_j \tilde{F}_{e_{k+m-j}}^{(Q)}) \tag{11}$$

where

$$\tilde{F}_{e_{k+m-j}}^{(Q)} = \frac{k_2 + 4k_2(\Omega^{(Q)})^2}{8\min\{2\mu_2, k_2/\sqrt{2}\} - \frac{16(\Omega^{(Q)}+F_e^{(Q)})}{(k+m-j)T - T_1}}$$

is a constant with T as the sampling time. The l-step-ahead prediction error is calculated by an iterative combination of one-step-ahead prediction errors.

D. Non-causal Linear Optimal Control with Adaptive Sliding Mode Observer

In this subsection, the NLOC is applied to maximize the energy output by using the predicted excitation force (10) and a compensation mechanism is embedded into the non-causal LOC to compensate for the prediction error whose boundary is estimated by (11).

The prediction error of the excitation force is defined as $\tilde{w} := w - \hat{w}$, where $\hat{w}$ is the excitation force prediction that is used by the non-causal LOC. The model (2) is then rewritten in the following form

$$\dot{x} = A_c x + B_{uc}u + B_{wc}\hat{w} + B_{wc}\tilde{w} \tag{12}$$

The first three terms on the right-hand side of (12) represent all the available information which can be used by the non-causal LOC for energy maximization, and the last term on the right-hand side of (12) represents all the unknown information which is to be handled by the compensator.

The nominal (disturbance-free) model of (12) is

$$\begin{cases} \dot{z} &= A_c z + B_{uc}v + B_{wc}\hat{w} \\ y_z &= Cz \end{cases} \tag{13}$$

where z and v are the nominal state and input. The nominal discrete-time model is

$$\begin{cases} z_{k+1} &= Az_k + B_u v_k + B_w \hat{w}_k \\ y_{zk} &= Cz_k \end{cases} \tag{14}$$

where the state matrices (A, B_u, B_w, C) are given in (3).

The proposed controller is

$$u = u_{LOC} + u_{SMC} \tag{15}$$

Ideally, when the perfect predictions are used by non-causal LOC, i.e. $u = u_{SMC} + K_x x + K_d w_{k,n_p}$, we have the following model

$$\dot{x} = A_c x + B_{uc}(u_{SMC} + K_x x + K_d w_{k,n_p}) + B_{wc}\hat{w} + B_{wc}\tilde{w} \tag{16}$$

The disturbance-free model of (16) is

$$\dot{z} = A_c z + B_{uc}(K_x x + K_d \hat{w}_{k,n_p}) + B_{wc}\hat{w} \tag{17}$$

Since the prediction error $\tilde{w}_{k,n_p}$ is not available, we prove that the proposed control policy (15) enables the ideal model (16) involving unavailable information to be approximated by the nominal model (17) which only uses known but inaccurate information.

The first term u_{LOC} of (15) is based on the non-causal LOC in [5], [22], which is designed as follows based on the nominal model (14)

$$u_{LOC} = K_x z_k + K_d \hat{w}_{k,n_p} \tag{18}$$

The second term u_{SMC} of (15) is the sliding mode controller used to cope with the prediction error by using the boundary of the prediction error (11), which is designed as

$$u_{SMC} = -\zeta \, \text{sgn}(s_c) \tag{19}$$

where $\zeta > 0$ is a constant satisfying the condition of

$$\zeta \geq \frac{\|GB_{wc}\|}{\|GB_{uc}\|}\max\{|\tilde{w}_{k+j|k}^{(Q)}|\} + 2n_p\|K_d\|\max\{|\tilde{w}_{k+j|k}^{(Q)}|\} \tag{20}$$

holds with $k = 0, 1, .., n_p - 1$ and the sliding variable is proposed as

$$s_c = G[x(t) - x(0) - \int_{t_0}^{t}(A_c x(\tau) + B_{uc}u_{LOC} + B_{wc}\hat{w}(\tau)$$
$$- n_p B_{uc}\|K_d\|\max\{|\tilde{w}_{k+j|k}^{(Q)}|\}\text{sgn}(s_c))d\tau] \tag{21}$$

which is a constant, and G is a vector with $8 + n_r$ elements such that GB_{uc} is invertible.

Theorem 1. *The prediction error is eliminated by the compensator* (19)*, and the dynamics of the ideal model* (16) *becomes the dynamics of the nominal model* (17)*.*

Proof: Choose a Lyapunov function as $V_{smc} = \frac{1}{2}s_c^2$, whose first time derivative is

$$\dot{V}_{smc} = s_c \dot{s}_c$$
$$\leq -\|s_c\|(\zeta\|GB_{uc}\| - (\|GB_{wc}\|\max\{|\tilde{w}_{k+j|k}^{(Q)}|\} \tag{22}$$
$$+ 2n_p\|GB_{uc}\|\|K_d\|\max\{|\tilde{w}_{k+j|k}^{(Q)}|\}))$$

Substituting (20) into (22), we have $\begin{cases} \dot{V}_{smc} < 0, & s_c \neq 0 \\ \dot{V}_{smc} = 0, & s_c = 0 \end{cases}$ holds for all s_c. Hence, the sliding mode $s_c = \dot{s}_c = 0$ is maintained. Considering that $s_c = \dot{s}_c = 0$ holds, we have the following dynamics

$$\dot{s}_c = G(\dot{x} - A_c x - B_c u_{LOC} - B_{wc}\hat{w}) = 0 \tag{23}$$

which yields

$$\dot{x} = A_c x + B_c u_{LOC} + B_{wc}\hat{w} \tag{24}$$

By substituting the nominal input $v = u_{LOC}$ into the nominal model (13), it can be found by comparison with (24) that the actual state x in the sliding mode becomes the nominal state z. Therefore, the dynamics of (13) and (24) becomes the same. ∎

Remark 3. *In practical implementations, the sign function in both ASMO and controller can be replaced by $f(x) = \frac{x}{\|x\| + d_c}$ with $d_c > 0$ as an arbitrary small constant to avoid chattering phenomenon.*

To avoid overlarge PTO torque, the gain of compensator is suggested to be selected as $\zeta = \frac{\|GB_{wc}\|}{\|GB_{uc}\|}\max\{|\tilde{w}_{k+j|k}^{(Q)}|\} + 2n_p\|K_d\|\max\{|\tilde{w}_{k+j|k}^{(Q)}|\}$.

IV. SIMULATION RESULTS

Wave profiles are of Joint North Sea Wave Project (JON-SWAP) form. The added mass m_∞ and the incoming excitation force are generated by a hydrodynamic software WAMIT [27]. The weighting matrices of the non-causal LOC are chosen as

$$Q_c = \begin{bmatrix} 0.1I_8 & 0_{8\times 8} \\ 0_{128\times 128} & 10^{-3}I_{128} \end{bmatrix}, \quad r = 0.08 \tag{25}$$

, as suggested in [22]. The sampling time is $T = 0.009$ s. The following 4 sets of simulation are done.

- Set 1: Performance degradation by insufficiently long prediction horizons and prediction errors
- Set 2: Comparison between the proposed control method and "non-causal LOC + Kalman Filter + AR" strategy proposed in [16]
- Set 3: Control performance with various sea-states
- Set 4: Design of prediction horizon n_p and control performance with different choices of ASMO parameters

A. Simulation Set 1: Performance degradation by insufficiently long prediction horizons and prediction errors

In this subsection, two factors degrading the control performance of non-causal LOC are investigated respectively. Firstly, perfect prediction of wave forces is assumed to demonstrate the performance degradation influenced by the length of prediction horizon; secondly, with a suitably chosen prediction horizon, several cases considering prediction errors are simulated to show the influences on control performance by the prediction error. We choose the values of significant wave height, the peakedness factor and the peak period as $H_s = 0.04$ m, $\gamma = 1$ and $T_p = 1.8$ s as suggested in [16], [22]. Since a 1:40 scaled model of M4 is used in simulation, the corresponding actual wave height is scaled to 1.6 m and the corresponding actual peak period is scaled to 11.4 s. A wide range of sea states are tested in Simulation Sets 2 & 3.

1) Performance degradation by prediction horizon length: The energy output of LOC with different wave prediction horizon lengths is shown in Fig. 4 to find the best choice of wave prediction horizon. The control performance degradation of non-causal LOC by insufficiently long prediction horizons is summarized in Table II.

TABLE II
ENERGY LOSS BY INSUFFICIENTLY LONG PREDICTION HORIZONS

Prediction horizon (s)	Energy output (J)	Energy loss (%)
$0 \times T_p$	12.6577	44.73%
$2 \times T_p$	20.2809	11.45%
$4 \times T_p$	21.7036	5.24%
$5 \times T_p$	22.9036	0.00%

TABLE III
CONTROL PERFORMANCE DEGRADATION BY PREDICTION ERRORS

Prediction error (%)	λ	Energy loss (J)	Energy loss (%)
5%	$\lambda = 1.001$	0.3613	2.31%
25%	$\lambda = 1.01$	1.0012	6.37%
35%	$\lambda = 1.02$	2.3789	15.14%
no prediction	-	4.6327	29.48%
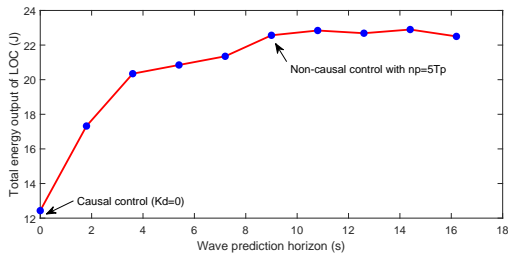
Fig. 4. Energy output after 100 s of LOC

It can be found from Fig. 4 that a suitable choice of the prediction horizon is $n_p = 5 \times T_p$, which achieves a good tradeoff between the prediction length and the WEC control performance. Table II quantifies the energy loss by different prediction horizon lengths.

2) Performance degradation by prediction errors: In this subsection, the prediction horizon is set to be $5 \times T_p$, which represents the best performance of the non-causal LOC. The prediction error of the wave excitation force is modelled as $\tilde{w}_k = L\tilde{w}_{k-1} + \xi_k, \quad k = 1, ..., 1000$, with $L > 1$. The filter is unstable matching prediction error in real scenario where it increases with the evolution of the prediction time. We choose $\xi_k \sim \mathcal{N}(0, 0.2)$ and $\tilde{w}_0 \sim \mathcal{N}(0, 0.5)$ as Gaussian white noises. The values of λ are chosen as $\lambda = 1.001$, $\lambda = 1.01$ and $\lambda = 1.02$, which are equivalent to 5%, 25% and 35% prediction errors, respectively. The energy output of non-causal LOC by different amplitudes of prediction errors is shown in Table III. It can be found in Table III that the prediction error degrades the control performance and is not negligible.

B. Simulation Set 2: Comparison between the proposed control method and "non-causal LOC + Kalman Filter + AR" strategy

To demonstrate the control performance of "non-causal LOC + Kalman Filter + AR" strategy proposed in [16], a wide range of simulations were run to obtain the capture width radio (CWR) of M4 with wave peak periods ranging from 0.7s to 1.8s with 0.1s interval, as shown in Fig. 5. The CWR is essentially non-dimensional power equal to the average power absorbed divided by wave power (incident
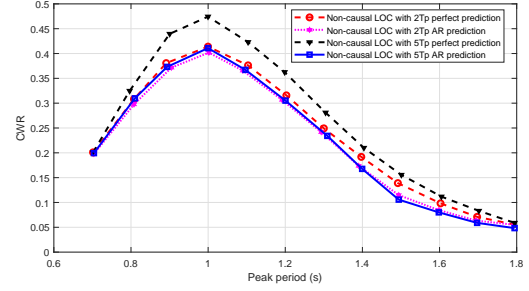

Fig. 5. CWR of "non-causal LOC + Kalman Filter + AR" strategy with wave excitation force prediction horizon as $2 \times Tp$ and $5 \times Tp$ ($H_s = 0.04$ m) [16]

power per metre crest) times wavelength of energy period (period corresponding to frequency of spectrum centroid) [23], [24].

As shown in Fig. 4, the best control performance of non-causal LOC is with a $5 \times T_p$ prediction horizon, while it is found in Fig. 5 that by using "non-causal LOC + Kalman + AR" strategy proposed in [16], the longest prediction ensuring an acceptable control performance is $2 \times T_p$. This is caused by two factors: 1) for the statistical method AR, prediction error of the excitation force grows as the prediction time grows; 2) wave force estimation errors by KF can affect the prediction accuracy, which in turn degrade control performance.

It can be found in [16] and [21] that the predictions of first 2 wave periods by both of strategies are accurate with 10.6% and 8.3% prediction errors respectively, while the predictions beyond 2 wave periods by both strategies are too large to be acceptable. Therefore, to achieve the best control performance by non-causal LOC which requires $5 \times T_p$ wave excitation force prediction, it is essential to design a SM compensator to compensate for both estimation and prediction errors. The control performance with and without SM compensation is compared in the case of $H_s = 0.04$ m and $T_p = 1.8$ s. Since the proposed "ASMO + improved AR" strategy enables us to explicitly calculate the estimation boundary and the prediction boundary, the gain parameter of SMC can be determined by (20). The energy output and power generated are shown in Fig. 6, which demonstrates that the effectiveness of the SM compensator on coping with the estimation and prediction error of excitation force. The trajectories of PTO torque with and without SM compensator are shown in Fig. 7, and Figs. 8 and 9 show the states of M4 device. It can be found that the proposed SM compensation based non-causal LOC does not increase the magnitude of PTO torque significantly, which means the proposed method ensures energy maximization subject to both estimation and prediction error without requiring extra PTO torque limit. Furthermore, the surge, heave, left pitch angle, right pitch angle and their velocities are barely affected, which ensures safe operations by using the proposed method.

C. Simulation Set 3: Control performance with various sea-states

To investigate the control performance in a wide range of sea states, the CWRs by the proposed control method and
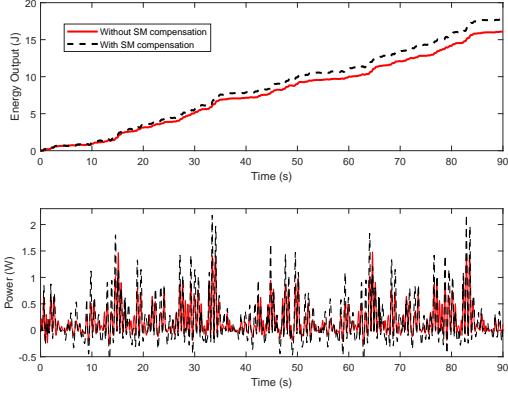
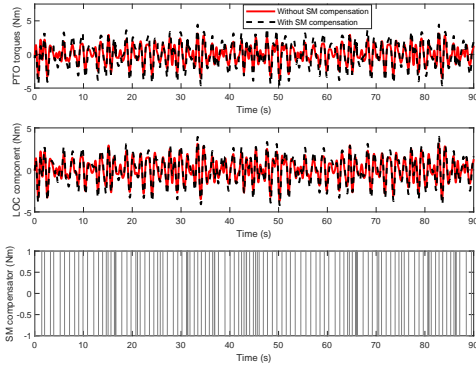Fig. 6.   Energy outputs and powers with and without SM compensation

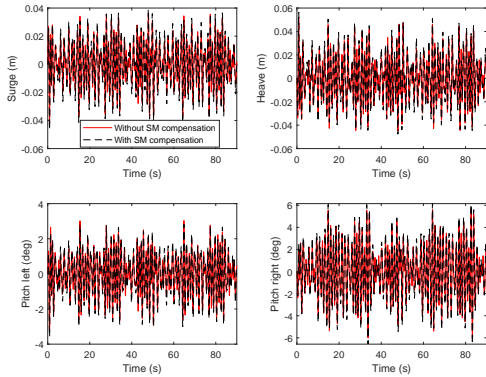Fig. 7.   PTO torques with and without SM compensation

Fig. 8.   Trajectories of surge, heave, pitch left and pitch right with and without SM compensation
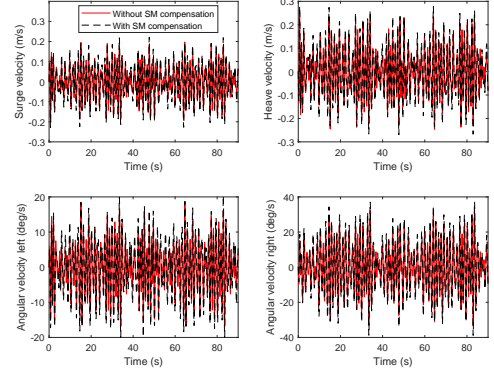

Fig. 9.   Trajectories of surge velocity, heave velocity, left angular velocity and right angular velocity with and without SM compensation
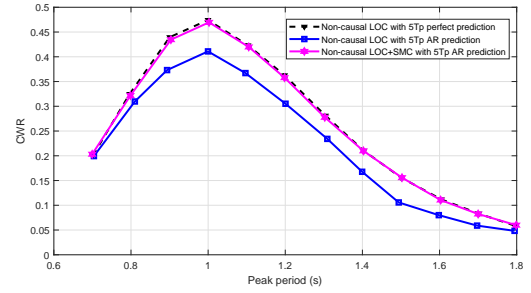

Fig. 10.   CWR of proposed control and control in [16] with prediction horizon as $5 \times Tp$

"non-causal LOC + Kalman Filter + AR" strategy [16] are shown in Fig. 10, in which wave height is fixed as $Hs = 0.04$ m. It can be found that the proposed SMC compensates for the estimation and prediction error effectively, by which the energy output is barely affected. Compared with the "non-causal LOC + Kalman Filter + AR" strategy [16], the proposed controller increases the energy output significantly.

Furthermore, irregular sea states with different wave heights ($H_s = 0.03$ m, $H_s = 0.05$ m and $H_s = 0.07$ m) are tested. With $5T_p$ AR prediction, the control performance of the method proposed in [16] without compensation and the proposed method with compensation is demonstrated by CWR. The CWRs of M4 with wave peak period ranging from 0.7s to 1.8s with 0.1s interval are shown in Fig. 11. It can be found that with the proposed compensator, a significant improvement on M4 energy conversion is achieved. Hence, the proposed method is verified to be effective in improving energy output without use of any extra hardwares to obtain prediction information. In addition, CWR should be unchanged by H_s as non-dimensional with constant damping, but CWR is not quite same with different H_s due to control and torque limit.

D. Simulation Set 4: Design of prediction horizon n_p and control performance with different choices of ASMO parameters

In this subsection, the choice of prediction horizon and different choices of parameters are tested to show how they influence the control performance.
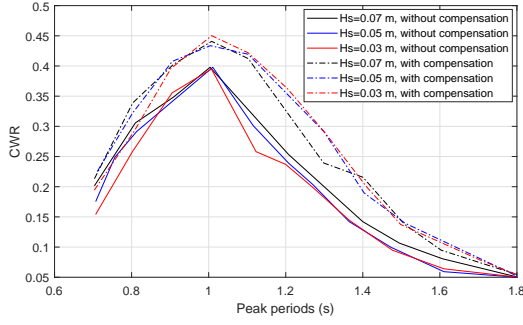
Fig. 11. CWR of proposed control (with compensation) and the control in [16] (without compensation) with prediction horizon as $5 \times Tp$
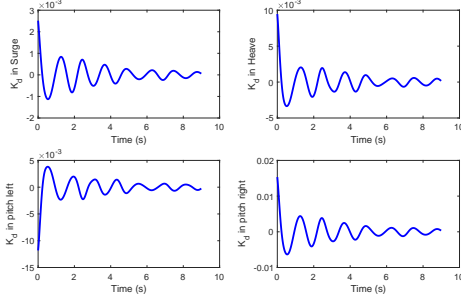

Fig. 12. Feed forward gain K_d in surge, heave, pitch mode, as prediction horizon proceeds

1) Design of prediction horizon n_p: Prediction horizon length is a key design parameter, which influences both control performance and computational load. It is discussed in Simulation Set 1 that insufficient length of prediction horizon n_p degrades the control performance. Thus n_p should be set as a large value as possible. However, it is also obvious from Fig. 12 that the gain K_d decreases to 0 as the prediction horizon becomes longer. Since K_d is fixed and independent of sea states, the incoming wave beyond 9 s (1000 step) does not significantly contribute to energy improvements. Hence, in practical applications of M4 device, whose sampling time is set to be 0.009 s in this paper, the prediction horizon is suggested to be $n_p = 1000$ for all sea states. For its application to other WECs, the prediction horizon needs to be tuned to find the best trade-off between the control performance and computational load.

2) Choices and tunings of ASMO parameters: The proposed method contains several ASMO parameters k_1, μ_0, α, μ_2 and k_2 in the observer. As discussed in Remark 2, k_1, μ_0 and α determines the length of warming-up period and does not affect the performance of the controller which starts to work thereafter. Therefore, in this subsection, we test control performance with different choices of parameters μ_2 and k_2. One sea state ($H_s = 0.04$ m and $T_P = 1.8$ s) is chosen as an example. To seek extreme value of the prediction error bound, wide ranges of k_2 and μ_2 are tested and the corresponding error bounds are calculated by Lemma 1. The results are shown in Fig. 13, in which the minimal error bound is found to be 1.0668 with $k_2 = 9.9$ and $\mu_2 = 3.5$. Hence, as calculated by (20), the minimal compensation gain is 1.038. The comparison

among control performance with different tuning of parameters is shown in Fig. 14. It can be seen that although the best choice $k_2 = 9.9$ and $\mu_2 = 3.5$ leading to the smallest error bound gives the best control performance, different parameter tuning does not significantly affect the control performance. Therefore, the proposed method is robust against the parameter tuning.
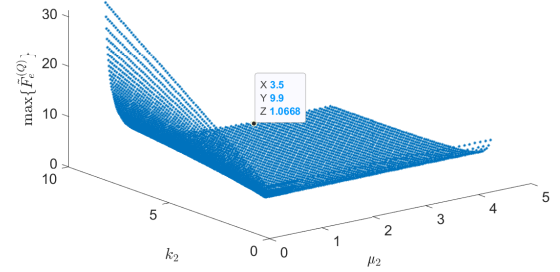

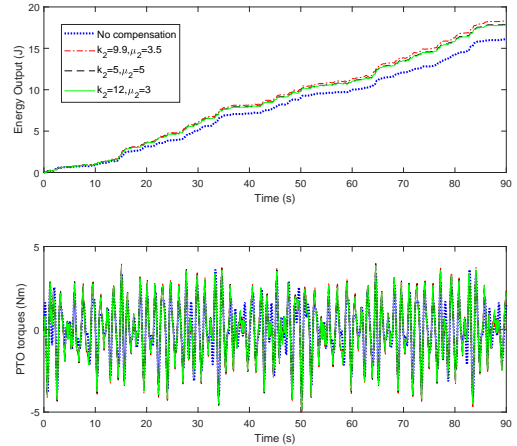Fig. 13. Error bounds to be used by the compensator

Fig. 14. Control performance with different choice of parameters

V. CONCLUSIONS

A non-causal linear optimal control with adaptive sliding mode observer strategy is proposed in this paper for energy maximization of WECs. Its main benefit is its enhanced robustness against the inevitable wave force prediction errors introduced by wave prediction techniques. An ASMO was applied to estimate the wave excitation force. With historical estimations, an improved AR method is used to predict incoming wave excitation force. A compensator is designed to deal with the prediction error. An attenuator type multi-float multi-motion WEC called M4 is adopted as a case study and the corresponding simulation results shows the effectiveness of the proposed control strategy. The control performance is not significantly affected by different parameters tuning of ASMO. The proposed control scheme can be straightforwardly extended to much wider WEC applications.

REFERENCES

[1] Raul Banos, Francisco Manzano-Agugliaro, FG Montoya, Consolacion Gil, Alfredo Alcayde, and Julio Gómez. Optimization methods applied to renewable and sustainable energy: A review. *Renewable and sustainable energy reviews*, 15(4):1753–1766, 2011.

[2] Benjamin Drew, Andrew R Plummer, and M Necip Sahinkaya. A review of wave energy converter technology, 2009.

[3] F de O Antonio. Wave energy utilization: A review of the technologies. *Renewable and sustainable energy reviews*, 14(3):899–918, 2010.

[4] Aurélien Babarit and Alain H Clément. Optimal latching control of a wave energy device in regular and irregular waves. *Applied Ocean Research*, 28(2):77–91, 2006.

[5] Siyuan Zhan and Guang Li. Linear optimal noncausal control of wave energy converters. *IEEE Transactions on Control Systems Technology*, 27(4):1526–1536, 2018.

[6] J Cretel, AW Lewis, G Lightbody, and GP Thomas. An application of model predictive control to a wave energy point absorber. *IFAC Proceedings Volumes*, 43(1):267–272, 2010.

[7] Jørgen Hals, Johannes Falnes, and Torgeir Moan. Constrained optimal control of a heaving buoy wave-energy converter. *Journal of Offshore Mechanics and Arctic Engineering*, 133(1):011401, 2011.

[8] Guang Li and Michael R Belmont. Model predictive control of sea wave energy converters–part 1: A convex approach for the case of a single device. *Renewable Energy*, 69:453–463, 2014.

[9] Romain Genest and John V Ringwood. A critical comparison of model-predictive and pseudospectral control for wave energy devices. *Journal of Ocean Engineering and Marine Energy*, 2(4):485–499, 2016.

[10] John V Ringwood, Giorgio Bacelli, and Francesco Fusco. Energy-maximizing control of wave-energy converters: The development of control system technology to optimize their operation. *IEEE Control Systems Magazine*, 34(5):30–55, 2014.

[11] Francesco Fusco and John V Ringwood. A study of the prediction requirements in real-time control of wave energy converters. *IEEE Transactions on Sustainable Energy*, 3(1):176–184, 2012.

[12] L Abusedra and MR Belmont. Prediction diagrams for deterministic sea wave prediction and the introduction of the data extension prediction method. *International Shipbuilding Progress*, 58(1):59–81, 2011.

[13] Marina Garcia-Abril, Francesco Paparella, and John V Ringwood. Excitation force estimation and forecasting for wave energy applications. *IFAC-PapersOnLine*, 50(1):14692–14697, 2017.

[14] Francesco Fusco and John V Ringwood. Short-term wave forecasting for real-time control of wave energy converters. *IEEE Transactions on Sustainable Energy*, 1(2):99–106, 2010.

[15] Yerai Peña-Sanchez, Marina Garcia-Abril, Francesco Paparella, and John V Ringwood. Estimation and forecasting of excitation force for arrays of wave energy devices. *IEEE Transactions on Sustainable Energy*, 9(4):1672–1680, 2018.

[16] Zhijing Liao, Peter Stansby, and Guang Li. A generic linear non-causal optimal control framework integrated with wave excitation force prediction for multi-mode wave energy converters with application to m4. *Applied Ocean Research*, 97:102056, 2020.

[17] Francesco Fusco and John Ringwood. A model for the sensitivity of non-causal control of wave energy converters to wave excitation force prediction errors. In *Proceedings of the 9th European Wave and Tidal Energy Conference (EWTEC)*. School of Civil Engineering and the Environment, University of Southampton, 2011.

[18] Yao Zhang and Guang Li. Non-causal linear optimal control of wave energy converters with enhanced robustness by sliding mode control. *IEEE Transactions on Sustainable Energy*, 2019, DOI: 10.1109/T-STE.2019.2952200.

[19] H-N Nguyen and Paolino Tona. Wave excitation force estimation for wave energy converters of the point-absorber type. *IEEE Transactions on Control Systems Technology*, 26(6):2173–2181, 2017.

[20] Mustafa Abdelrahman and Ron Patton. Observer-based unknown input estimator of wave excitation force for a wave energy converter. *IEEE Transactions on Control Systems Technology*, 2019. DOI: 10.1109/TC-ST.2019.2944329.

[21] Yao Zhang, Tianyi Zeng, and Guang Li. Robust excitation force estimation and prediction for wave energy converter m4 based on adaptive sliding-mode observer. *IEEE Transactions on Industrial Informatics*, 2019, DOI: 10.1109/TII.2019.2941886.

[22] Zhijing Liao, Nian Gai, Peter Stansby, and Guang Li. Linear non-causal optimal control of an attenuator type wave energy converter m4. *IEEE Transactions on Sustainable Energy*, 2019, DOI: 10.1109/T-STE.2019.2922782.

[23] Peter Stansby, Efrain Carpintero Moreno, and Tim Stallard. Large capacity multi-float configurations for the wave energy converter m4 using a time-domain linear diffraction model. *Applied Ocean Research*, 68:53 – 64, 2017.

[24] Peter Stansby, Efrain Carpintero Moreno, and Tim Stallard. Capture width of the three-float multi-mode multi-resonance broadband wave energy line absorber m4 from laboratory studies with irregular waves of different spectral shape and directional spread. *Journal of Ocean Engineering and Marine Energy*, 1(3):287–298, 2015.

[25] R Eatock Taylor, PH Taylor, and PK Stansby. A coupled hydrodynamic–structural model of the m4 wave energy converter. *Journal of Fluids and Structures*, 63:77–96, 2016.

[26] L Sun, J Zang, Peter Stansby, E Carpintero Moreno, PH Taylor, and R Eatock Taylor. Linear diffraction analysis of the three-float multi-mode wave energy converter m4 for power capture and structural analysis in irregular waves with experimental validation. *Journal of Ocean Engineering and Marine Energy*, 3(1):51–68, 2017.

[27] You-Hong Eng, Cheng-Siong Chin, and Michael Wai-Shing Lau. Added mass computation for control of an open-frame remotely-operated vehicle: Application using wamit and matlab. *Journal of Marine Science and Technology*, 22(4):405–416, 2014.

Yao Zhang received her Ph. D. in Department of Control Science and Engineering, Harbin Institute of Technology in 2018. She is currently a Lecturer in Northumbria University. She was a postdoctoral researcher in Queen Mary University of London. Her research interest covers sliding mode control, model predictive control and applications on aerospace, marine engineering and renewable energy.

Peter Stansby is the inaugural Osborne Reynolds Professor of Fluid Mechanics in the School of Mechanical, Aerospace and Civil Engineering (MACE) in the University of Manchester and Fellow of the Royal Academy of Engineering. In a long career to date spanning 40 years, he has been a Dynamicist at Atkins Research and Development, a member of the W.S. Atkins Group, a Lecturer, Senior Lecturer, Professor of Hydrodynamics at the Engineering Department of the Victoria University of Manchester, Head of the Manchester Centre for Civil and Construction Engineering, UMIST, Professor of Hydrodynamics in MACE and Head of the School of MACE. Of relevance to this paper he has been developing wave energy devices for a decade through experiments and linear wave/body modelling resulting in the patented multi-float modular system M4.
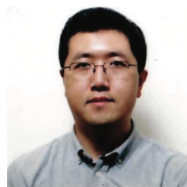
Guang Li received his Ph.D. degree in Electrical and Electronics Engineering, specialized in control systems, from the University of Manchester, in 2007. He is currently a senior lecturer in dynamics modelling and control in Queen Mary University of London, UK. His current research interests include constrained optimal control, model predictive control, adaptive robust control and control applications including renewable energies and energy storage, etc.